Mechanisms of dropwise condensation on aluminum coated surfaces

To cite this article: Matteo Mirafiori *et al* 2022 *J. Phys.: Conf. Ser.* **2177** 012046

Mechanisms of dropwise condensation on aluminum coated surfaces

Matteo Mirafiori[1], Marco Tancon[1], Stefano Bortolin[1], Alessandro Martucci[1], Davide Del Col[1*]

[1] University of Padova, Department of Industrial Engineering
Via Venezia 1, 35131 Padova, Italy

[*]Corresponding author e-mail: davide.delcol@unipd.it

Abstract. Dropwise condensation (DWC) is a complex phase-change phenomenon involving the formation of randomly distributed droplets on the condensing surface. The promotion of DWC instead of the traditional filmwise condensation (FWC) is a promising solution to enhance the efficiency of heat exchangers by increasing the condensation heat transfer coefficient. The interaction between the condensing fluid and the surface (wettability) is important in defining the condensation mode. On metallic surfaces widely employed in heat transfer applications, the condensing process occurs in filmwise mode. Ideally, an engineered surface designed to achieve high DWC heat transfer coefficients should present low contact angle hysteresis and low thermal resistance. Among the different available techniques to modify the surface wettability, hybrid organic-inorganic sol-gel silica coatings functionalized with hydrophobic moieties (phenyl or methyl groups) have been identified as a feasible solution to promote DWC on metallic surfaces. In the present paper, different aluminum sol-gel coated surfaces have been tested during DWC of steam in saturated conditions. The realized coatings have been characterized by means of dynamic contact angles and coating thickness measurements. Condensation tests have been performed using a two-phase thermosyphon loop operating in steady-state conditions that allows visualization of the condensation process and simultaneous heat transfer measurements. Heat transfer coefficients have been measured by varying the heat flux, at 106 °C saturation temperature and with vapor velocity equal to 2.7 m s^{-1}. A high-speed camera is used for the visualization of the DWC process.

1. Introduction

Water vapor condensation is a two-phase heat transfer process encountered in many engineering applications as thermal power plants, heat pipes, sea water desalinization and buildings heating/cooling systems. An improvement in the efficiency of the condensation process can have a significant effect on the reduction of energy consumptions. Researchers have identified dropwise condensation (DWC) as a potential solution for enhancing the efficiency of the filmwise condensation (FWC) heat transfer process. During classic FWC of pure steam, the presence of a continuous liquid film which forms in correspondence of the heat exchanger walls contributes to the main thermal resistance. On the contrary, DWC involves the formation of discrete droplets and their rapid removal is entrusted by an external force (e.g. gravity or vapor drag force). The heat transfer coefficient (HTC) during DWC is usually 5−7 times higher as compared to the one measured during filmwise condensation [1].

The interaction between the surface and the condensing fluid plays a crucial role in determining the condensation mode (filmwise or dropwise). Coatings that are able to promote DWC over metallic substrates usually present the following characteristics: low surface energy compared to the surface tension of the condensing fluid (for this reason is more difficult to achieve DWC with low surface tension fluids) and high droplet mobility. For the evaluation of droplet mobility, the sessile drop method can be used to measure dynamic contact angles (advancing θ_a and receding θ_r contact angle): a small difference between the advancing and the receding contact angle, named contact angle hysteresis $\Delta\theta$, is associated to high droplet mobility.

DWC is a quasi-cyclic process with characteristic timescales, fraction of the surface covered by droplets, and drop-size distribution [2]. DWC begins at the molecular scale with droplets nucleation in preferred sites. Drops grow by direct condensation at first and later by coalescence until they reach the critical dimension at which the external forces (e.g., gravity, vapor drag) overcome the retention forces and they start to move. Sliding droplets sweep the surface and make new nucleation sites available. Since the renewal mechanism is directly affected by the droplet mobility, promoting droplets sweeping was found to increase the heat transfer coefficient of the DWC process [3].

Thanks to the promising heat transfer enhancement given by DWC and to the availability of new surface coatings, research is nowadays focused on both experimental investigation (heat transfer measurements, visual observations of the droplet population) and mathematical modelling of the DWC. The models are aimed at describing all the processes involved during DWC: the nucleation of a drop, its growth until its departure, the heat exchanged by the drop during its lifetime, the droplet removal and the resulting population of the droplets on the surface. In particular, droplets population can be divided in two parts: the small droplet population characterized by droplets growing by direct steam condensation and the large droplet population in which the coalescence between neighbors drops is the dominant growing mechanism [4]. For the large droplets population, the droplet sizes distribution was proposed by Rose[1].

As demonstrated by several authors [4], the heat transferred through a single droplet is the result of several thermal resistances. In particular, the presence of a coating used to modify the wettability of the metallic surface introduces an additional thermal resistance that in turn depends on the thickness of the coating and on the thermal conductivity (and thus on the chemistry of the coating). When the coating thermal resistance is not negligible, the resulting overall heat transfer coefficient will be lower and the advantage given by DWC can be reduced as reported in Parin et al. [5].

In the present work, DWC of steam has been experimentally investigated on three different aluminum sol-gel coated surfaces. Heat transfer coefficients measurements and visualizations of droplets population have been performed at a constant vapor velocity of 2.7 m s^{-1} and varying the heat flux between 70 and 550 kW m^{-2}. The recorded high-speed videos have been analyzed by using a home-made MATLAB® program with the aim to link the droplet dynamic to the heat transfer coefficient for the different coated substrates.

2. Experimental setup

The experimental apparatus used for condensation tests is a two-phase thermosiphon loop which consists of a boiling chamber, a test section, a cooling water circuit, and a post-condenser. The layout of the experimental test rig is shown in Fig. 1a. Steam, which is generated in the boiling chamber by means of electrical heaters (with a maximum power of 4 kW), enters the test section in saturated conditions and it is partially condensed over a vertical aluminum sample (condensing area 50 mm high by 20 mm wide). The surface of the sample exposed to the condensing steam (front side) is coated with a sol-gel silica layer. To obtain continuous condensation in the test section, heat is removed from the back side of the sample by using chilled water provided by an external thermal bath at a controlled flow rate and inlet temperature. Vapor condensation inside the pipeline between the boiling chamber and the test section is avoided by using electrical resistance wires to balance the heat losses through the ambient. Downstream the test section, the two-phase mixture enters a post-condenser where the vapor is fully condensed and subcooled. The subcooled liquid returns to the boiler chamber driven by the buoyancy force due to the difference between the liquid and the vapor density and it closes the circuit.

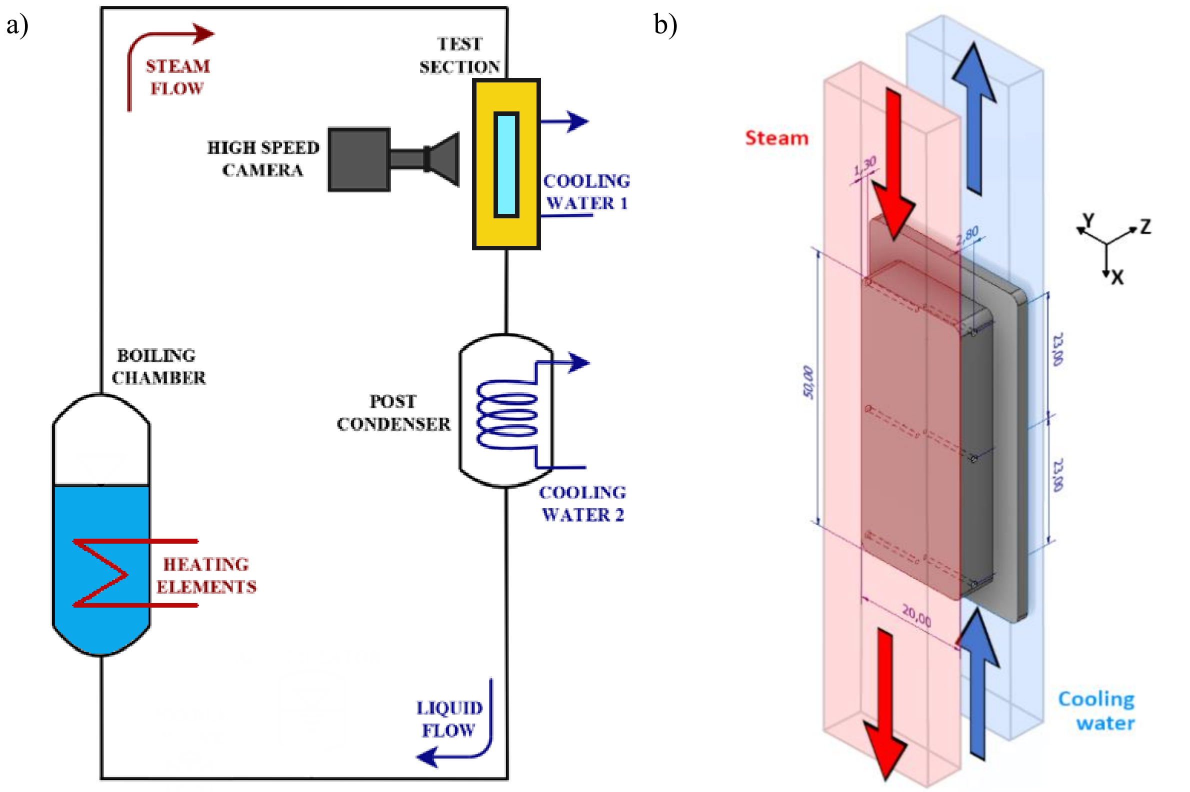

Figure 1. Experimental apparatus: a) schematic view of the thermosiphon loop; b) 3D model of the test section and the aluminum sample (dimensions in mm). Orientation of *x*-*y*-*z* axis is also shown.

The average condensation heat flux over the surface is obtained from the coolant mass flow rate $\dot{m}_{cool}$ and the temperature difference measured at the inlet and outlet of the test section ΔT_{cool} as follows:

$$q_{mean} = \frac{\dot{m}_{cool}\, c_{cool}\, \Delta T_{cool}}{A} \tag{1}$$

In Eq. (1), c_{cool} is the specific heat capacity of the coolant and A is the area of the condensing surface. Six thermocouples are placed inside the metallic specimen at two different depths from the condensing surface (z_1 = 1.3 mm and z_2 = 2.8 mm) and in correspondence of three longitudinal positions x along the sample (Fig. 1b). Starting from the thermocouples temperature measurements, the Fourier's law can be applied to obtain the surface temperature ($T_{wall,loc}$) for each of the three longitudinal positions:

$$T_{wall,loc} = T_{z_1} + \left(T_{z_1} - T_{z_2}\right)\frac{z_1}{z_2 - z_1} \tag{2}$$

In Eq. (2), T_{z_1} and T_{z_2} are the temperatures measured at depths z_1 and z_2 respectively. The three local values of surface temperature $T_{wall,loc}$ are then averaged over the whole condensing area to obtain the mean value of the HTC:

$$\mathrm{HTC} = \frac{q_{mean}}{T_{sat} - T_{wall}} \tag{3}$$

where T_{sat} is the saturation temperature of the steam. The thermodynamic and transport properties of the steam are evaluated by means of NIST Refprop version 10.0 [6]. Each experimental data reported in this work is the mean of 480 readings acquired at 1 Hz and the uncertainty bars are calculated with a coverage factor k = 2. Additional information about the test rig, the measuring technique and the procedure for the evaluation of the experimental uncertainty are reported in Parin et al. [7].

3. Experimental results and discussion

Condensation tests have been performed in steady-state conditions and varying the heat flux from 70 to 550 kW m^{-2}, while maintaining a constant steam velocity (≈ 2.7 m s^{-1}), saturation temperature (≈ 106 °C) and coolant mass flow rate (0.11 kg s^{-1}). High-speed videos have been recorded at a constant value of heat flux (≈ 440 kW m^{-2} as show in Fig. 2a) in order to investigate the effect of the coating on droplets mobility. Experimental data have been obtained on three aluminum samples treated with different sol-gel coatings: coating #1 (Parin et al. [5]), coatings #2 and #3 (Parin et al. [7]). The three surfaces have been characterized by means of dynamic contact angle measurements using the sessile drop method and by coating thickness measurements. The results of surface characterization are summarized in Table 1. After functionalization, the three surfaces showed a nearly hydrophobic behavior with advancing contact angle $\theta_a \approx 90°$ and receding contact angle $\theta_r \approx 60°$. According to the work proposed by Cha et al. [8], the reduced contact angle hysteresis (Table 1) improves droplet mobility and it allows to promote DWC even on surfaces with relatively low advancing contact angle (e.g. below 90°). With the aim to avoid possible changes of surface wettability due to the exposure in harsh environment, the samples have been tested for approximately 2 hours, which is a time interval shorter if compared to the coating lifetimes.

Table 1. Advancing and receding contact angles, contact angle hysteresis and coating thickness for the three investigated sol-gel coatings.

	θ_a [°]	θ_r [°]	$\Delta\theta$ [°]	δ_{coat} [nm]
Coating #1 [5]	89 ± 1	64 ± 3	25 ± 2	250 ± 5
Coating #2 [7]	83 ± 3	57 ± 6	26 ± 5	300 ± 25
Coating #3 [7]	87 ± 3	64 ± 2	23 ± 3	420 ± 35

In Fig. 2, the effect of the heat flux on the HTC during DWC is presented for the three coated aluminium samples. As shown in Fig. 2a, the saturation-to-wall temperature differences (ΔT) increases almost linearly with the heat flux and therefore the HTC remains nearly constant over the whole range of wall subcooling here investigated (Fig. 2b). The performed experiments showed that dropwise condensation can be sustained on the aluminum samples realizing thermal fluxes up to 500 kW m^{-2} with a temperature difference between saturation and wall below 6 K. On the contrary, in order to obtain a similar heat flux (≈ 400 kW m^{-2}) during filmwise condensation (FWC), the temperature difference would be around 30 K [9]. With coatings #2 and #3, the HTC is almost 5 to 6 times higher as compared to the HTC measured during FWC in similar conditions.

The sample treated with coating #1 exhibits the highest values of the HTC (between 180 and 190 kW m^{-2} K^{-1}) while, for coatings #2 and #3, the measured HTCs are significantly lower, with values that are in the range 85-100 kW m^{-2} K^{-1}. It must be pointed out that, considering the present experimental technique, the measured HTC takes into account the thermal resistances due to condensation process [4] plus the thermal resistance of the coating. The latter is strongly influenced by the thickness of the coating as deeply discussed in [5]. In particular, the thermal resistance associated with the conduction through the coating increases with the thickness of the coating. As it will be shown in the following analysis, the difference in the HTCs measured with the three coatings can only be partially explained by the different thickness of the DWC promoter layer (considering the same value of thermal conductivity for all the three sol-gel coatings). In order to predict the effect of the coating layer thermal resistance on the HTC, the dropwise condensation model by Kim and Kim [4] was considered. The thermal resistances per unitary area were calculated as the ratio of the film thickness (see Table 1) to the coating thermal conductivity λ supposed equal to 0.2 W m^{-1} K^{-1}. Considering that the wettability is almost the same for the three coatings (Table 1) as well as the other input parameters needed for the application of the model, the calculated HTC is affected only be the coating thermal resistance, which is higher for coating #2 and #3 (30% and 70% respectively as compared with coating #1 thermal resistance ≈ 1.32 K MW^{-1}). The HTC predicted for coating #1 is respectively increased by 10% and 25% as compared to the HTC calculated for coatings #2 and #3. Therefore, as shown in Fig. 2, the HTC increase measured with coating #1 is not only due to the lower thickness of the coating.

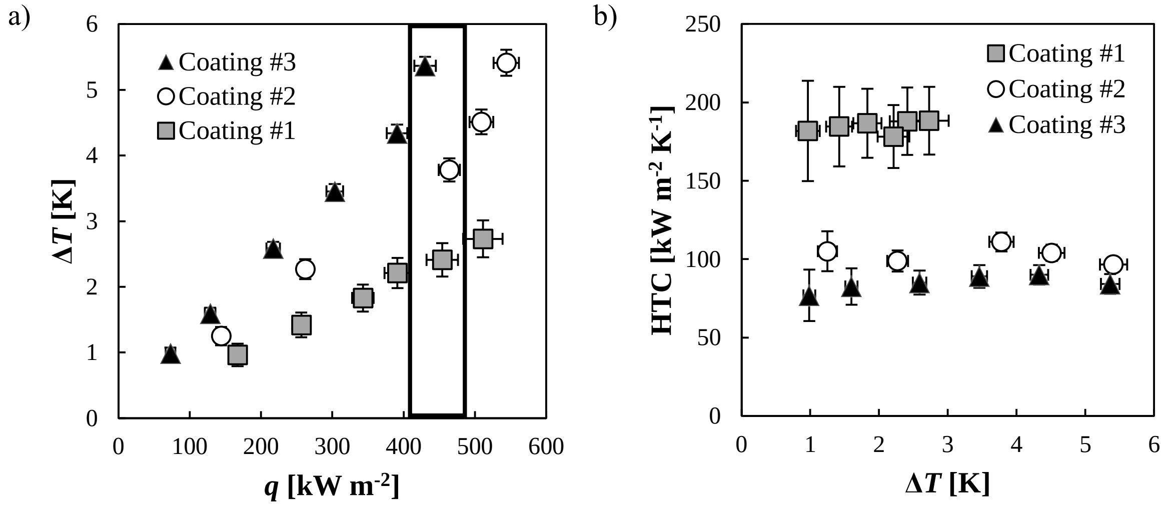

Figure 2. a) Saturation-to-wall temperature difference ($\Delta T = T_{sat} - T_{wall}$) versus heat flux ($q$) and b) heat transfer coefficient (HTC) versus temperature difference ΔT measured during DWC tests on the three aluminum samples (named coating #1, coating #2 and coating #3).

As a second step, heat transfer measurements are analysed considering also droplets dynamics. In order to study the droplets mobility, in particular to investigate the surface renewal time, the recorded videos were analysed to evaluate the fraction f of the surface area covered by droplets, which was firstly introduced by Rose [1]. Considering the droplets detection threshold of the present optical technique, the fraction f is determined from Eq. 4 as reported in Parin et al. [7]

$$f = \frac{A_c}{A_{tot}} \quad (4)$$

where A_c is the area of the condensing surface occupied by drops with radius greater than 200 µm (which represents the recognition threshold) and A_{tot} is the total investigated area which is the same for the three samples analysed (≈ 2.85 cm^{-2}). It must be noted that, in the present work, the parameter f is evaluated considering only a fraction of the large droplet population since the video acquisition system (which consists of a LED plus a high-speed camera Photron FASTCAM UX100 coupled with a macro-lens) allows to detect droplets down to 200 µm radius [7]. When f approaches to unity it means that the inspected area is almost entirely covered by drops whereas, when f is equal to zero, it means that there are no visible drops in the inspected area with radii larger than 200 µm. With the aim of evaluating the f parameter, each recorded frame extracted from the high-speed videos has been analysed using a home-made MATLAB® program for droplet recognition. The program allows to detect both the position and the radius of the droplets within the inspected area. A detailed description of the MATLAB® program can be found in [7].

The three graphs in Fig. 3a show the evolution against time of the fraction area f measured considering the three different samples. The analysis has been performed at a constant heat flux of ≈ 440 kW m^{-2} and with a fixed time interval equal to 1 s. For coating #1, the evolution of the fraction area with time (graph on the left in Fig. 3a) has been linked to the images of the droplet population reconstructed using the MATLAB® program (Fig. 3b). From the experimental data, it results that f can be described as a periodic function with its characteristic amplitude and frequency. Higher the amplitude and the frequency of the f function, shorter the surface renewal time and more efficient the sweeping mechanism that makes new nucleation sites available. The surface renewal frequency for coating #1 is around 1.8 Hz and this value results respectively 20% and 35% higher than the measure one for coating #2 and #3 (Fig. 3a). As expected, when the fraction area f reported in Fig. 3a is compared against HTC measurements (Fig. 2b), a higher surface renewal frequency corresponds also to higher values of the HTC. Looking at the amplitude of the f function, it can be observed that, despite of the similar surface renewal time, the amplitude for coating #2 is higher compared to the amplitude measured for the coating #3: this means that the sweeping mechanism cleans larger portions of the investigated area in the case of the coating #2, making the droplet renewal process more efficient.

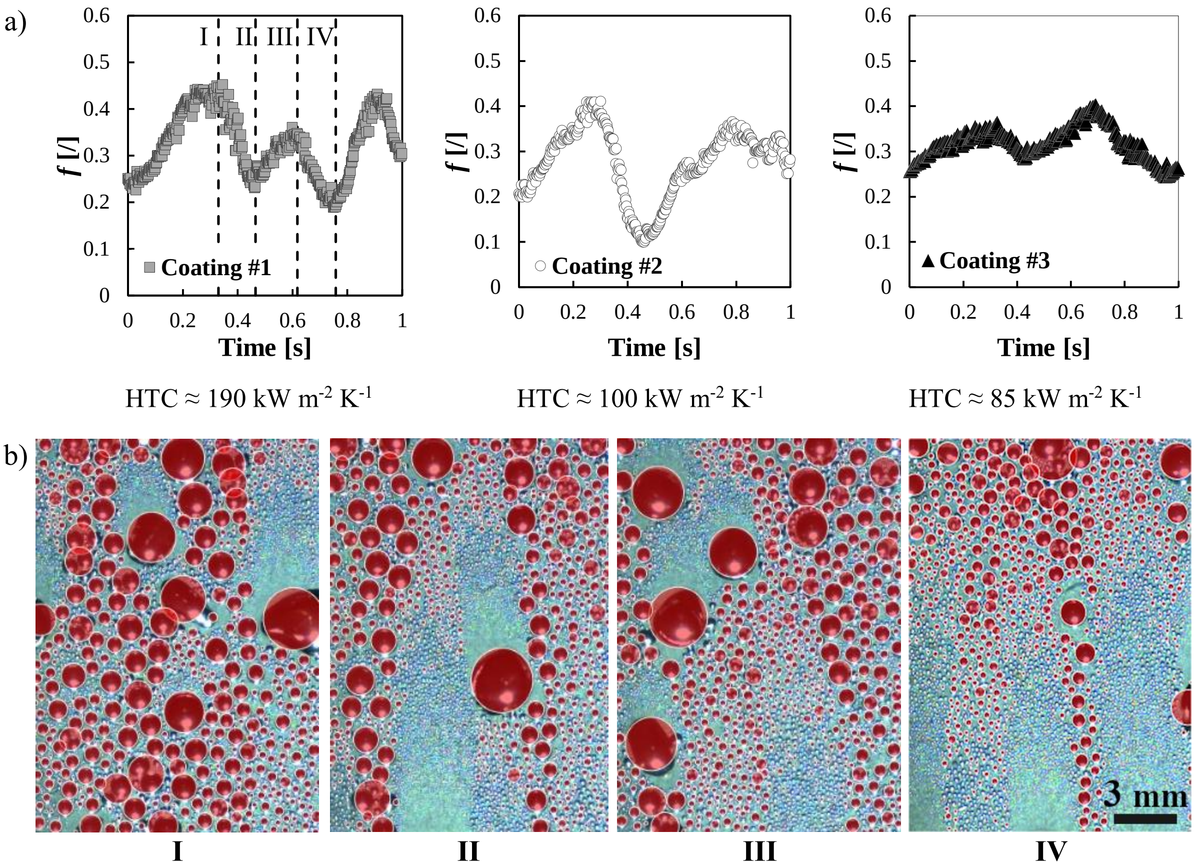

Figure 3. a) Fraction area f occupied by droplets with radii higher than 200 μm plotted versus time for the coatings #1, #2 and #3 (heat flux ≈ 440 kW m^{-2}, inspected area ≈ 2.85 cm^2). For each coating, the corresponding value of the measured HTC is also reported. b) Time evolution of the droplets population on the sample with coating #1. The resulting image after video analysis and droplet recognition by MATLAB® program (red transparent circles) is superimposed to the original image taken by the high-speed camera.

From the video analysis, it is possible to obtain the sweeping period (τ) that, according to the work by Kim and Kim [4], can be expressed as the ratio of the selected area to the sweeping rate at which the surface is renewed by falling drops. Therefore, it indicates the time necessary for renewing the whole surface. The sweeping period was calculated evaluating the maximum and minimum peak of the fraction area f. In fact, the variation Δf between a maximum of the parameter f (e.g. at time step I in Fig. 3a) and the following minimum (at time step II in Fig. 3a) corresponds to a certain portion of the sample surface that was renewed up to that time instant. Thus, the sweeping period can be calculated as the ratio between the observation time interval (e.g. 1 s) and the sum $\sum \Delta f$ of the fraction area variations between a maximum and next minimum, measured in the same observation time interval. The results obtained with the three coatings show that the sweeping period for coating #1 is 1.7 s, whereas DWC on coatings #2 and #3 is respectively characterized by sweeping periods of 2.5 s and 4.2 s. As expected, the highest HTC was measured with the coating exhibiting the lowest sweeping period. It must be considered that the sweeping period calculated with the present method accounts for surface renewal due to coalescence with sliding droplets (droplets that have reached the departure diameter) whereas it does not account for surface renewal due to coalescence between static droplets (droplets that do not have yet reached the departing diameter) as reported in the work by Lethuilleir et al. [10].

4. Conclusions

In the present paper, HTC measurements and droplets dynamic analysis during DWC of steam have been presented for three different sol-gel coated aluminum samples. The three coatings displayed similar wettability ($\theta_a \approx 90°$ and $\theta_r \approx 60°$) but different coating thickness (in the range between 250 ÷ 420 nm). Condensation tests have been performed at constant saturation temperature (≈ 106 °C) and steam velocity (≈ 2.7 m s^{-1}), while varying the heat flux between 70 kW m^{-2} and 550 kW m^{-2}.

All the three coated samples sustained DWC with HTCs considerably higher than the values measured during FWC. In particular, the HTC measured with coating #1 was the highest (≈ 185 kW m^{-2} K^{-1}), while the HTCs measured with coatings #2 and #3 were respectively around 100 and 85 kW m^{-2} K^{-1}. The effect of the additional thermal resistance due to the thickness of the coating was estimated using the DWC model by Kim and Kim [4]. The predicted overall HTC for coating #1 results to be increased by 25% compared to coating #3 due to the lower thickness of the sol-gel coating. However this does not fully explain the higher HTC values measured with coating #1.

Images of the droplets population evolution taken with a high-speed camera have been analysed by a home-made software in MATLAB® code and the following parameters have been determined: the time evolution of the fraction area f occupied by droplets and the sweeping period τ. From the measurements, the sweeping period measured over coating #1, which exhibited the highest HTC, was found to be lower than the value measured with the other two coatings.

Acknowledgements

The authors acknowledge the financial support of the Department of Industrial Engineering, University of Padova through the BIRD187743 project. The support of the European Space Agency through the MAP Condensation program ENCOM (AO-2004-096) is also acknowledged.

References

[1] J. W. Rose, “Dropwise condensation theory and experiment: A review,” *Proceedings of the Institution of Mechanical Engineers, Part A: Journal of Power and Energy*, vol. 216, no. 2, pp. 115–128, Jan. 2002, doi: 10.1243/09576500260049034.

[2] B. S. Sikarwar, K. Muralidhar, and S. Khandekar, “Effect of Drop Shape on Heat Transfer During Dropwise Condensation Underneath Inclined Surfaces,” *Interfacial Phenomena and Heat Transfer*, vol. 1, no. 4, pp. 339–356, 2014, doi: 10.1615/interfacphenomheattransfer.v1.i4.30.

[3] M. Tancon, R. Parin, S. Bortolin, A. Martucci, and D. Del Col, “Effect of steam velocity during dropwise condensation,” *International Journal of Heat and Mass Transfer*, vol. 165, p. 120624, 2021, doi: 10.1016/j.ijheatmasstransfer.2020.120624.

[4] S. Kim and K. J. Kim, “Dropwise Condensation Modeling Suitable for Superhydrophobic Surfaces,” *Journal of Heat Transfer*, vol. 133, no. 8, p. 081502, 2011, doi: 10.1115/1.4003742.

[5] R. Parin, M. Sturaro, S. Bortolin, A. Martucci, and D. Del Col, “Heat transfer during dropwise condensation of steam over a mirror polished sol-gel coated aluminum substrate,” *International*

Journal of Thermal Sciences, vol. 144, pp. 93–106, Oct. 2019, doi: 10.1016/j.ijthermalsci.2019.05.017.

[6] E. W. Lemmon, I. H. Bell, M. L. Huber, and M. O. McLinden, "NIST Standard Reference Database 23: Reference Fluid Thermodynamic and Transport Properties-REFPROP, Version 10.0, National Institute of Standards and Technology." 2018, doi: https://dx.doi.org/10.18434/T4JS3C.

[7] R. Parin, M. Tancon, M. Mirafiori, S. Bortolin, L. Moro, L. Zago, F. Carraro, A. Martucci, and D. Del Col, "Heat transfer and droplet population during dropwise condensation on durable coatings," *Applied Thermal Engineering*, vol. 179, no. January, p. 115718, 2020, doi: 10.1016/j.applthermaleng.2020.115718.

[8] H. Cha, H. Vahabi, A. Wu, S. Chavan, M. K. Kim, S. Sett, S. A. Bosch, W. Wang, A. K. Kota, and N. Miljkovic, "Dropwise condensation on solid hydrophilic surfaces," *Science Advances*, vol. 6, no. 2, 2020, doi: 10.1126/sciadv.aax0746.

[9] A. Bisetto, S. Bortolin, and D. Del Col, "Experimental analysis of steam condensation over conventional and superhydrophilic vertical surfaces," *Experimental Thermal and Fluid Science*, vol. 68, pp. 216–227, Nov. 2015, doi: 10.1016/J.EXPTHERMFLUSCI.2015.04.019.

[10] J. Lethuillier, P. Lavieille, and M. Miscevic, "About the Role of Falling Droplets' Sweeping in Surface Renewal during Dropwise Condensation," *Langmuir*, vol. 36, no. 43, pp. 12877–12886, Nov. 2020, doi: 10.1021/acs.langmuir.0c02092.